

PRESENT STATUS OF BOOSTER SYNCHROTRON UTILIZATION FACILITY AT KEK

H. Sasaki

National Laboratory for High Energy Physics
Oho-machi, Tsukuba-gun, Ibaraki, 305, Japan

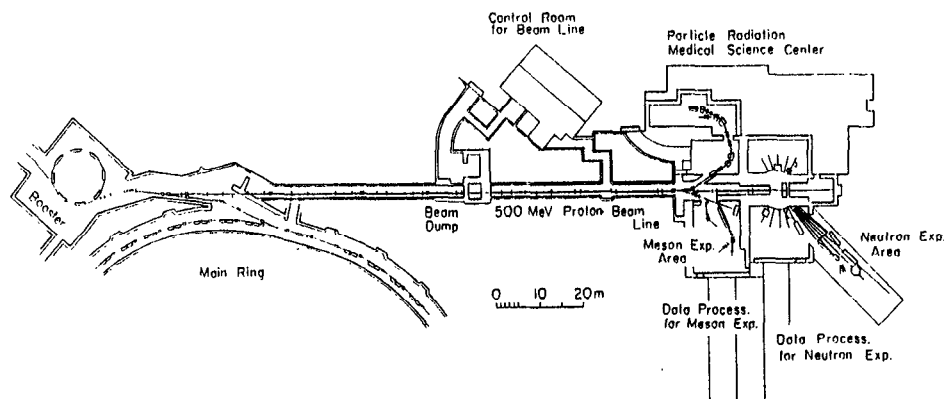


Fig. 1 Layout of Booster Synchrotron Utilization Facility

Introduction

Booster Synchrotron Utilization Facility BSF at KEK was established in 1978 in order to organize a neutron scattering experimental facility KENS, a pulsed muon facility BOOM and a biomedical facility PARMS. Those facilities utilize the proton beam from the 500 MeV booster for 12 GeV Proton Synchrotron. The neutron scattering experimental facility and the pulsed muon facility came into operation in the early summer of 1980, and the biomedical facility in June 1982. Figure 1 shows the layout of BSF at KEK. The 20 Hz booster synchrotron delivers about 40 beam pulses to BSF every 2.5 sec at an average beam intensity of 5 to 6×10^{11} protons/pulse as shown in Fig. 2. BSF has been operated for a total of 8,950 hrs and at an operating efficiency of more than 90 % since June 1980, as shown in Table 1. Most of the beam time in BSF is shared equally by the neutron scattering experiment and the pulsed muon experiment. For instance, the neutron scattering experimental facility KENS has been operated for a beam time of 1,509 hrs in the fiscal year 1982. Shortage of the beam time for the physics research program becomes more serious because BSF has started to deliver proton beams to the new biomedical facility in

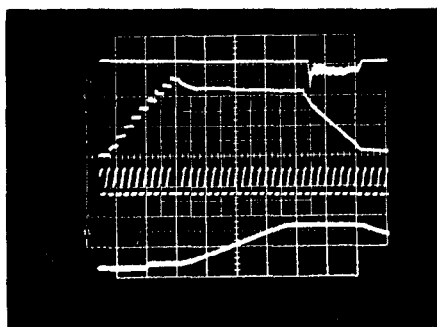


Fig. 2 Extracted 12 GeV proton beam, circulating proton beam in 12 GeV main ring synchrotron, circulating beam current in 500 MeV booster, and magnetic field of main ring synchrotron. (from upper to lower) 200 ms/div.

Table 1 BSF Operation Summary

Fiscal Year (April-March)	Accelerator Operating Time (hr)	Total Operating Time (hr)	BSF Operation Efficiency (%)	Beam Time for Neutron Experiment (hr)
1980	3,533	1,628	89.9	926
1981	3,258	2,883	93.0	1,422
1982	3,652	3,219	95.0	1,509
July 1983	1,432	1,218	95.0	516
Total	11,875	8,948	93.4	4,373

addition to a steady increase of the number of users in the physics research program.

Accelerator System

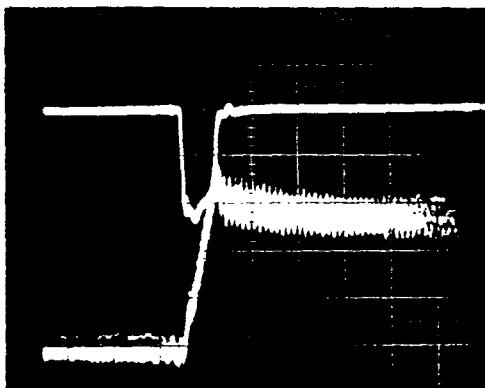
Present Status

A 100 mA, 5 μ sec wide proton beam is fed into the booster synchrotron from a 20 MeV injector linac at the repetition rate of 20 Hz. Figures 3(a) and (b) show the circulating proton beam at around injection and during the acceleration, respectively. In usual, the beam transmission in the booster synchrotron is some 25 %. The stability of the output beam intensity is quite satisfactory as shown in Fig. 4.

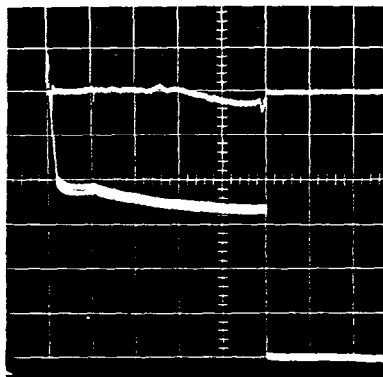
Since 1980, the booster synchrotron began to deliver the beam to BSF as well as the 12 GeV main ring synchrotron with its full capacity. Recently, therefore, the residual radioactivities at off-time of the accelerator became more serious problem to maintenance and improving works. On the other hand, there are no indications of the increase of failure hours due to the full operation of the booster synchrotron as shown in Table 2.

Conversion of Injection Scheme in Booster

The physics research programs in BSF as well as those of high energy physics in KEK demand more beam. A scheme of H^- charge-exchange injection has been considered as a powerful candidate to meet such demands. The conversion from the present multi-turn injection of proton beam to the charge-exchange injection makes possible to not only increase the



(a) 5 μ sec/div.



(b) 5 msec/div.

Fig. 3 (a) Injected Linac Beam: 50 mA/div.
Circulating Beam in Booster: 125 mA/div.
(b) Radial Position of Circulating Beam.
Circulating Proton Beam: 2×10^{11} protons/div.

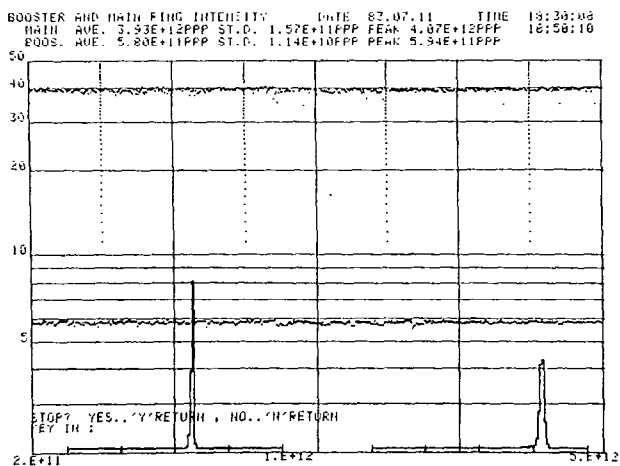


Fig. 4 Beam Intensity Fluctuation of Booster and Main Ring Synchrotron

Table 2 Failure Time of Accelerator Component (hrs)

Fiscal Year	Pre-Injector	Linac	20 MeV Beam Line	Booster Magnet	Booster RF	Extraction & 500 MeV Beam Line
1979	14.2	23.4	17.2	4.7	17.7	41.5
1980	9.2	24.5	1.6	14.5	9.2	10.8
1981	23.1	26.8	2.1	7.9	2.0	15.2
1982	9.1	26.3	16.8	7.1	3.2	28.4

intensity of the proton beam but also to reduce considerably beam loss in the booster. In addition, an appreciable polarized proton beam would be accelerated in the synchrotron by such an injection scheme. The conversion program to the scheme of the charge-exchange injection started on 1979 together with a project of acceleration of polarized proton beam in KEK PS.

Arrangement of the H^- ion beam injection system is shown in Fig. 5. Four orbit bump magnets, each of which is 340 mm long with a useful aperture of 160 mm(H) x 40 mm(V), are excited to 0.24 T by a 7 kA, 100 μ sec current pulse. Carbon foils of 30, 50 and

120 μ g/cm² in thickness will be available for the charge stripper. Including a spare-foil mounting device with housing capacity of 40 foils, almost components of the injection system have been completed and are ready for installation.

Development of the H^- ion source started with the construction of a magnetron-type surface plasma ion source¹⁾. Under suitable operating conditions, more than 30 mA H^- ion beam was obtained²⁾. However, it became clear that there were some technical problems on the life time of the ion source itself, stability and control of ion beam in the source, etc. Therefore, conversion to another type of ion source has been considered. At present, a prototype of cusp or bucket H^- ion source³⁾ is under construction. In this type of the ion source, converter is separated from the cathode and those can be controlled independently.

The second RF cavity was introduced into the booster ring and has been examined. The RF system together with both of cavities has become more stable and reliable in its operation. This will be a powerful means of compensation for the beam loading due to the expected increased beam current in the charge-exchange injection.

Charge-exchange injection will be tested with polarized H^- and unpolarized H^- ions in this October.

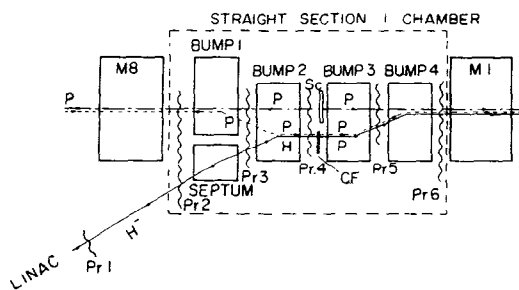


Fig. 5 Charge-exchange Injection System of Booster H^- : Injected H^- ions.
P: Circulating proton beam.
BUMP 1 ~ 4: Orbit bump magnet.
Pr 1 ~ 6: Multi-wire profile monitor.
CF: Carbon foil charge stripper.
Sc: Beam scraper.

Extension of Injector Linac⁴⁾

If the energy of the present 20 MeV injector linac is doubled, the beam intensity of the booster synchrotron will be considerably increased in connection with the adoption of charge-exchange injection. Next year, 1984, construction of the large tunnel for an electron-positron colliding storage ring, TRISTAN, and hence shut-down of the 12 GeV proton synchrotron is scheduled. It is under planning to upgrade the linac energy in this term.

While the space for the second linac tank will be available in the present beam line to the booster without difficulty, there is no room for new high power RF source. In the present 20 MeV linac, the operating beam current is 150 mA and its beam power is 3 MW. As the excitation power of the tank is about 1 MW, the total power of 4 MW is shared by two TH516 amplifier tubes. If 30 mA H⁺ ion beam is assumed to be accelerated to 40 MeV, the total power including the excitation power of the tanks is 3.2 MW, which is less than that of the present operating mode with proton beam. The present two feed system for RF power, will be also adopted in the second tank. This has not only good RF characteristics for beam loading compensation but also a practical advantage. Even if one of the TH516 amplifier system is completely down, the linac will be able to run with a lower beam current.

Parameters of the second tank for the 40 MeV linac is listed in Table 3.

Table 3 Main Parameters of the Second Tank for 40 MeV Linac

Energy	20.40 - 40.48 MeV
Frequency	201.070 MHz
$\beta\lambda$	0.3060 - 0.4244 m
$\beta^2\gamma^3$	0.04491 - 0.09195
Tank	Steel, copper plated
Length	12.82 m
Inside diameter	0.90 m
Number of cells	35
Drift tube	Stainless steel, copper plated
Outer diameter	16 cm
Bore diameter	3 cm
Quadrupole magnet	permanent (ALNICO-9)
Aperture	3.4 cm
Length	16 cm
Outer diameter	13.5 cm
Field gradient	2.2 - 2.25 kG/cm
Synchronous phase	-30°
Average axial field	2.2 MV/m
Shunt impedance	74.34 - 72.51 M Ω /m
Transit time factor	0.8519 - 0.7915
Effective shunt impedance	53.95 - 45.43 M Ω /m
Excitation power	0.845 MW
Beam power (for 30 mA)	0.60 MW
Total RF power	1.445 MW
RF coupling	Loop, two feeds
Stabilizer	Post couplers
Vacuum system	
Main pump	Ion pump (1,000 l/s x 8)
Auxiliary pump	Turbomolecular pump (500 l/s x 2)
Temperature regulation	$\pm 0.1^\circ\text{C}$

Neutron Scattering Experimental Facility (KNES)

Numbers of neutron scattering experiments have been carried out with the 5 spectrometers of the HIT, MAX, LAM, SAN and TOP, as well as new members of machine, such as FOX (four circle single crystal diffractometer), PEN (polarized epithermal neutron spectrometer), CAT (crystal analyzer TOF spectrometer), RAT

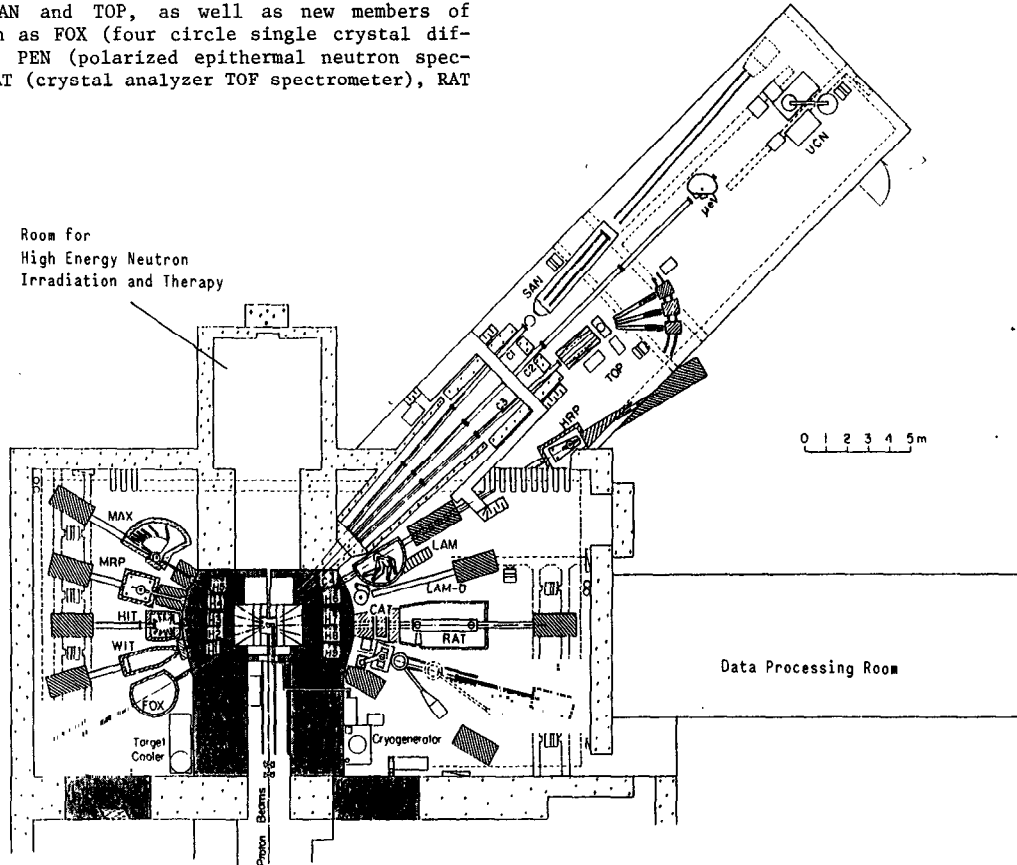


Fig. 6 Layout of the Spectrometers in KENS

(resonance detector TOF spectrometer), and LAM-D, which opened to the user community. Consequently 10 spectrometers have been operated. In fact the number of research proposal to the BSF increases steadily, but the total machine time reached the maximum and is rather decreasing recently because the beam time shared with Particle Radiation Medical Science Center is increasing. For instance, more than 100 specimens of glasses, amorphous materials and liquids have been measured with the HIT diffractometer, but several proposals are still in a waiting list.

Two powder diffractometers HRP (high resolution powder diffractometer) and MRP (medium resolution powder diffractometer) are under construction in reply to the users' strong requests. A new high resolution quasi-elastic spectrometer LAM-80 is also under construction based on a prototype experiment already achieved. Figure 6 shows the recent layout of the spectrometers.

Neutron Source

The pulsed spallation neutron source, KENS, was operated satisfactorily throughout FY 1982. The total

operation time was 1,509 hours. The second target of W installed at the beginning of this period is still in operation without any serious radiation damage. Since the first target suffered serious erosion with the condensation of NO_x gas generated by radiations, the second target is situated in a gas free environment.

As the first step of the KENS-I' project we have obtained an appreciable gain in cold neutron flux by changing a solid methane moderator with a grooved surface. After the extensive studies of both experiments at the Hokkaido linac and computer simulations at JAERI to optimize, we have installed a new grooved moderator replacing the previous flat one at the end of FY 1982. Then we confirmed the gain factor of about 1.4 which was just expected from the results of design studies. Figure 7 shows the neutron spectrum from the new grooved moderator compared to that from the previous flat one. The time structures of cold neutrons at various energies are also shown in Fig. 8, which represent an elongation of pulse width with a small preceding pulse from the teeth of the grooved surface. Pulse broadening themselves are not so serious even for the quasi-elastic spectrometer such as LAM-40 and LAM-80. Photograph of the new grooved moderator is shown in Fig. 9. Details are given in a separate article in this meeting).

As the second step the preparation of a depleted uranium target system is under progress. The development and fabrication of a prototype rectangular uranium target block and the fabrication of the first set of blocks (4 pieces) for KENS-I' use have already been ordered to Argonne National Laboratory. The blocks will be supplied by the end of March 1984. The target has been designed to accept an up-upgraded proton beam current of 10 μ A.

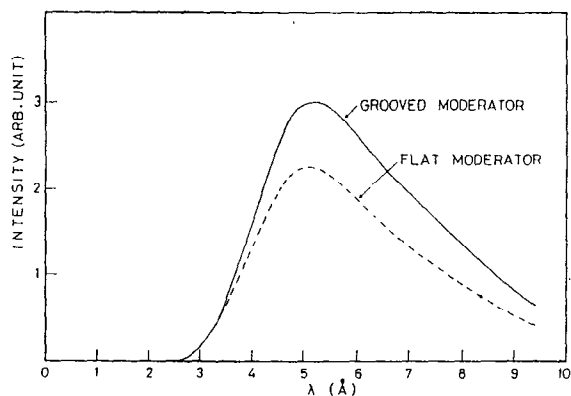


Fig. 7 Neutron Spectrum Extracted from the New KENS Grooved Solid Methane Moderator (20 K) (Solid Line). Compared dotted curve is that of the previous flat one.

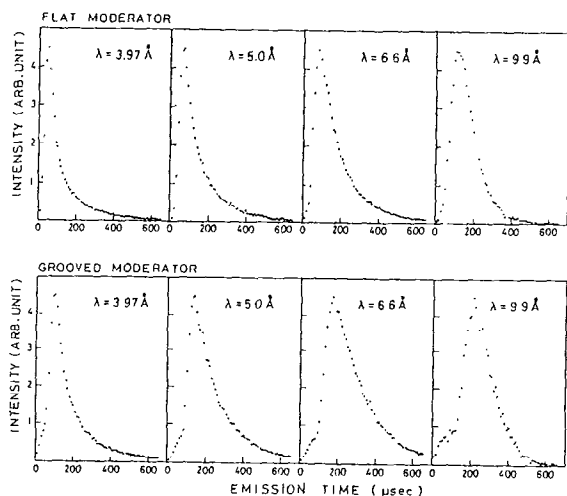


Fig. 8 Pulse Profiles in Time Scale of Cold Neutrons from Grooved and Flat Solid Methane Moderators at Various Wave Lengths



Fig. 9 View of New KENS Grooved Moderator

Neutron Scattering Experiments

Among many experiments conducted since last ICANS meeting, several topics are selected and described very briefly in this report. The more detailed results are seen in the KENS Report IV⁶⁾.

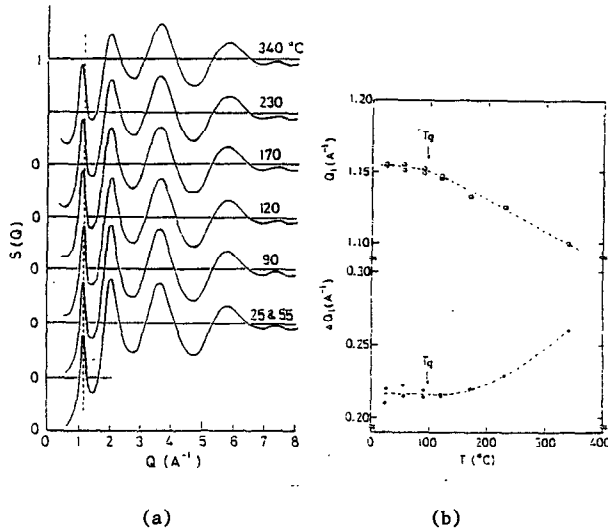


Fig. 10 (a) Temperature Variation of the Structure Factor, and (b) the Peak Position and the Peak Width of the First Peak at $Q=1 \text{ \AA}^{-1}$, in P_2Se_3 below and above the Glass Transition Temperature (100°C)

As was mentioned in the preceding section the HIT is the busiest machine in this facility. The well determined resolution components and wide range of the momentum transfer Q enable us to investigate the precise short range or partial structure factor $S(Q)$ of the topological disordered materials. One of the remarkable examples shown here is the structural change associated with the glass transition of the P_2Se_3 glass at 100°C . As is demonstrated in Fig. 10(a), the variation of the structure factor is remarkable in the first peak near 1 \AA^{-1} in Q . More quantitatively the peak position and the width of the first peak in Q vary above the glass transition temperature and are frozen immediately at this transition temperature, which is shown in Fig. 10(b). The present result provides the first experimental evidence which clarifies the correlation between the glass transition temperature and the structural change at the glass transition of the glass materials.

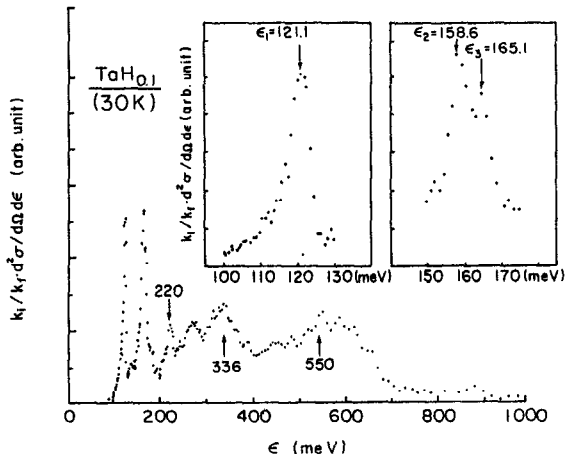


Fig. 11 Local Mode Spectrum for $TaH_{0.1}$ at 30 K. Inserted figures are those in enlarged scale near the first excited levels.

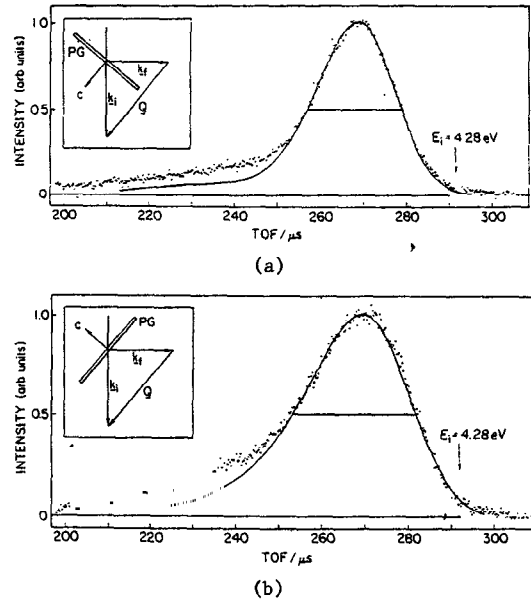


Fig. 12 High Q Scattering Spectra from Pyro-graphite for (a) $Q // C$ and (b) $Q \perp C$

It has been recognized that the pulsed neutron scattering method is superior in high energy regions of sub eV or eV energy, and such experiments to demonstrate high quality investigation are performed with the RAT and CAT spectrometers. Utilizing the time focussing principle the energy resolution of the CAT reaches as small as 3% for 1 eV energy transfer. This highest resolution spectrometer in the world is suitable to elucidate the dynamics of light elements such as H_2 , Be, C, etc. embedded in the transition metals and alloys. For instance the energy splitting in the first excited energy levels of the hydrogen local modes in $TaH_{0.1}$ was well observed for the first time, which has long been considered to be degenerated (Fig. 11). The experimentally determined energy levels are also interpreted by the crystalline distortion to the orthorhombic from the cubic symmetry due to the hydrogen doping. Inelastic scattering studies at high momentum transfer Q have also been elucidated using a resonance detector technique. Numbers of technical developments have been achieved currently and a detailed line profile is able to be analyzed. Curves shown in Fig. 12 are examples looking at the scattering from the pyrolytic graphite crystal. The line widths of modes parallel and perpendicular to the C plane differ approximately by a factor of 1.5. This result is qualitatively interpreted by the fact of the mode difference of density of states of phonons.

Significant parts of activities in the neutron scattering research at KENS facility are concerned with the low energy neutron spectroscopy using the solid methane moderator. It has long been believed that the pulsed cold neutron source cannot compete with the cold neutron source at steady state reactor, and an important question has been raised whether any experiment better than those using the latter source may be performed. Several examples selected from the outcomes using the KENS cold neutron source are considered to be the answer.

Neutron quasielastic spectra of polymers, aqueous solutions, etc. have been extensively studied with the LAM-40 spectrometer. Very recently the high resolution has been attained down to less than $20 \mu\text{eV}$ with a new developed machine of LAM-80. Eventually the combination of both LAM-40 and -80 spectrometers enable us to

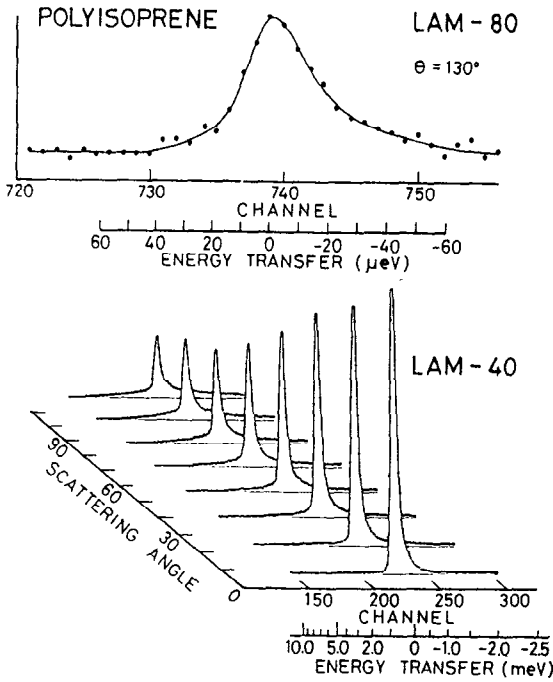


Fig. 13 Quasielastic Neutron Inelastic Spectra of Butadiene Observed by LAM-40 and LAM-80

elucidate the details of molecular or polymer diffusion processes due to the achievement of the high resolution and the wide energy transfer. A typical example obtained in this way is diffusion motions in butadiene of the commercial rubber: Looking at the quasielastic neutron spectra with the two different spectrometers as shown in Fig. 13, we are aware of existence of two types of diffusions characterized by two relevant relaxation times, τ_1 and τ_2 . According to the de Gennes model, the results are interpreted as that the fast diffusion ($\tau_1 \sim 10^{-12}$ sec) corresponds to the rotational diffusion mode inside the polymer pipe due mainly to thermal fluctuations of bonding angles and that the slow motion ($\tau_2 \sim 5 \times 10^{-11}$ sec) corresponds to the jump mode along the pipe.

The small angle camera (SAN) installed at an end of the guide tube viewing the cold source contributes to many users in the research fields of polymer science, biology, metallurgy and solid state physics. The SAN has also a unique feature utilizing the full advantage of the pulse technique. Besides the coverage of the wide momentum space due to the wide band of incoming neutron wave length, the time evolution of the structure analysis can easily be performed. Consequently extensive efforts have been directed to physics of nonequilibrium state, such as problems of spinodal decomposition, spin glass transition, etc. Collecting enormous amounts of data points stored in the 2 mega bites bulk memories, time transient pictures can be taken in various time scales. As an example the response of the magnetic short range order in a spin glass material of $(\text{FeTiO}_3)_{0.88}(\text{Fe}_2\text{O}_3)_{0.12}$ to the pulsed magnetic field, which is projected on the crystalline a^*c^* plane, is shown in Fig. 14. These pictures depict how the magnetic clusters appearing in the zero field behave in the applied field. It seems to indicate the nonlinear growing process of such magnetic clusters. On the other hand the slower relaxation processes have been elucidated using FeCr alloys which show a well known spinodal decomposition. The successful interpretation has been obtained by a recent nonlinear theory

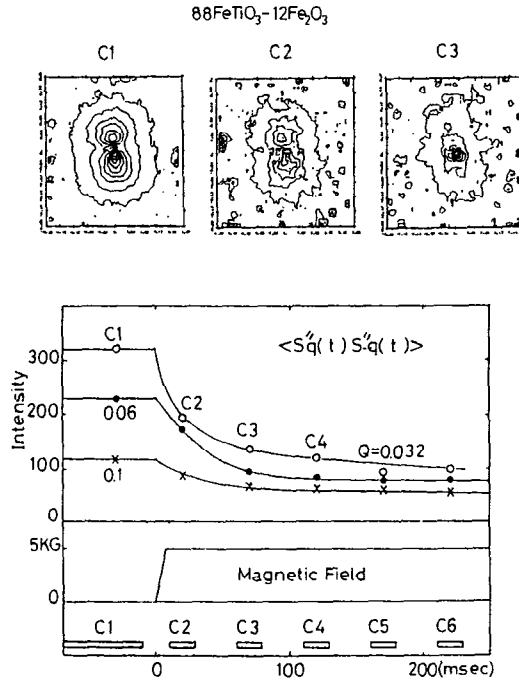


Fig. 14 Two Dimensional Display of Time Dependent Response of Magnetic Clusters in $(\text{Fe}_2\text{O}_3)_{0.12}(\text{FeTiO}_3)_{0.88}$ Spin Glass

due to the fact that we could observe the detailed time evolution of diffraction in the wide Q range.

The TOP provides polarized pulse neutrons with continuous wave length longer than 3 Å. Besides the magnetic structure analysis for herimagnets with a long period, amorphous magnets, composite magnetic multi-layers and fine particles, the dynamical polarization analysis is one of current topics. Wave length dependence of depolarization of transmitted polarized neutrons through a ferromagnetic thin plate was directly measured for the first time since Halpern and Holstein studied theoretically long time ago (1941). We applied this technique to the study on spin dynamics in random ferromagnets often called as spin glasses. In these materials the randomness is so strong that the ferromagnetic order may be destroyed. In other words the spin fluctuating frequency may become slow in these

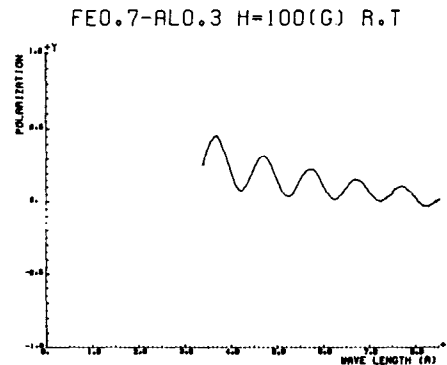


Fig. 15 Wave Length Dependence of Depolarization of Transmitted Polarized Neutrons through FeAl Spin Glass

materials and the neutron scattering cannot detect such low frequencies of the spin dynamical part. As is shown in Fig. 15, polarization of transmitted neutrons through a FeAl spin glass changes with the wave length considerably. The decrease of polarization with respect to the wave length is interpreted by introduction of the random field. If the random field is assumed to be stochastic, the neutron spins with the longer wave length spend longer time in the random field resulting more depolarization. The oscillation represents existence of a stationary field resulting the Larmor oscillation of the neutron spins.

To conclude this section we emphasize that numbers of experiments have been performed, a part of which is significant to yield scientific impacts and others are useful to develop new technique. Besides these examples just shown before, many other significant outcomes have been obtained by the MAX, PEN, FOX, LAM-D, and UCN spectrometers.

Instrumental Development

A High Resolution Powder diffractometer HRP is being installed at a position about 18 m from the cold source (downstream the LAM-40 spectrometer on the C-4 beam line). This instrument utilizes sharp pulses of thermal neutrons from the solid methane moderator at 20 K and a resolution $\Delta d/d \sim 0.002$ is expected with backward counters at $2\theta \sim 170$ deg. A Medium Resolution Powder diffractometer MRP is under construction at H-4 beam hole viewing the room temperature moderator. The instrument is designed to provide a higher counting rate but with a medium resolution $\Delta d/d = 0.007 \sim 0.02$.

Considerable progress has been achieved in the polarized epithermal neutron spectrometer PEN and an electron volt spectrometer RAT. The higher proton polarization more than 70 % has been achieved with PEN which stands far above the corresponding value of 45 % with a prototype experiment by Pre-PEN. Extensive studies on the resonance detector foil have been carried out and the best detector resolution $\Delta E_r \sim 50$ meV ($\Delta E_r/E_r = 0.75\%$) at $E_r = 6.67$ eV has been attained by an uranium foil cooled down to 25 K.

A prototype experiment for a higher resolution quasi-elastic spectrometer LAM-80 has attained higher energy resolution better than 20 μ eV. The instrument utilized a similar analyzer mirror as LAM-40 but with $\theta_B \sim 80^\circ$. LAM-80 is equipped with four analyzer mirrors at any scattering angles and being installed at the end of the C-2 guide tube.

Finally the guide tube of C-2 is extended by 6 m, and consequently the total flight path is now going to be 29 m from the source to the end of C-2 guide. Several UCN experiments and high resolution spectroscopy in the sub μ eV energy region will be considered from the beginning of FY 1984.

Pulsed Muon Facility BOOM⁵⁾

Meson Science Laboratory was born in 1978, attached to Faculty of Science of the University of Tokyo, to conduct basic research in science using mesons, in particular, as the first step, to build a meson facility BOOM at the KEK booster synchrotron utilization facility BSF. The final goal of this experimental facility is to construct high quality pulsed muon experimental facility and to conduct research project based upon the maximum use of the time structure of the pulsed proton beam from the 500 MeV booster synchrotron. The beam has a suitable time structure of 50 nsec pulse width and 50 msec separation. Such a pulsed beam can be quite effectively coupled with the extreme experimental condition which can be realized only with a low duty factor such as a high RF field, a high power laser, etc.

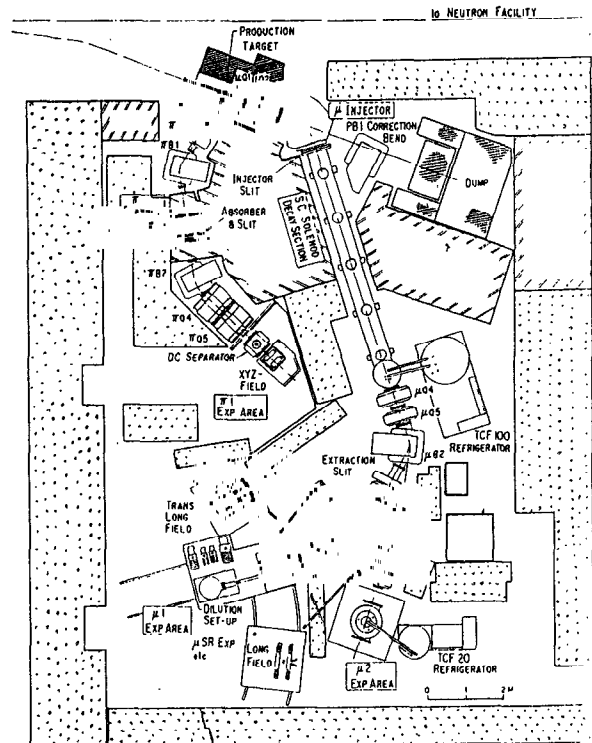


Fig. 16 Layout of Pulsed Muon Facility BOOM

Layout of the pulsed muon facility is shown in Fig. 16.

Since the first operation of the superconducting muon channel in July 1980, the superconducting solenoid and its cooling system has already marked over 7,000 hrs running time in almost maintenance-free mode. The $\mu 1$ port attached to the superconducting channel has been in use for the wide varieties of pulsed muon experiments by taking high quality backward muons. Table 4 is a summary of the muon beam properties at $\mu 1$. The $\mu 2$ muon extraction channel is used as either alternative channel for backward muons sharing beam time with $\mu 1$ port or simultaneous operational channel for forward muons. A parasite pion channel with take-off angle of 102.5° from incident proton beam is mainly used as a surface muon channel. At present, it is possible to have surface μ^+ at the $\mu 1$ port with an intensity of $10^5 \mu^+$ /sec in an area of 12 cm x 2 cm.

Almost the experiments conducted in BOOM are based on the techniques of μ SR. The μ SR method, utilizing asymmetric emission of e^- along polarized muon spin, can be used to probe the local magnetic field and its fluctuation felt by the muon inside various condensed

Table 4 Summary of Muon Beam Properties at $\mu 1$ Port

		Case 1	Case 2
$p\pi$	(MeV/c)	$200 \pm 5\%$	$150 \pm 5\%$
$p\mu$	(MeV/c)	≈ 110	≈ 75
Stopping Range Width	(g/cm ²)	3.5	2.0
Intensity	(μ^+ /pulse)	35 K	28 K
	(μ^+ /sec)	700 K	560 K
Polarization		80 %	80 %
Spot Area FWHM	(cm x cm)	5 x 5	5 x 5

Table 5 List of Active Experiments in BOOM
(April 1982 - March 1983)

Exp. No.	Title (Abridged) Actual Subject	Beam Time (h)		
		μ^1/μ^2 (BWD)	μ^2 (FWD)	π^1
M 1	μ -channel tuning Forward μ^- tuning Forward μ^+ test		168 146	
M 2	μ -channel tuning DC separator tuning Muonium detection development Gas phase muonium formation test Fion tuning			262 224 77 31
M 3	Pulsed μ SR developments Polyacetylene test REAR ₂ compound test GaP semiconductor test	22 33 5		138
M 4	μ^+ & μ^- in H ₂ O Decoupling & decoupling resonance	83		
M 5	μ^+ SR on Ni Critical phenomena	100	30	
M 8	Muonium in hydrocarbon Decoupling & decoupling resonance Muonium spin rotation	83 42		55
M10	Average polarization of ¹² B after μ^- capture on ¹² C Testing, long-run and after-check	421		
M11	μ^+ SR defects in metals ZF- μ SR on AlMg alloys			77
M12	Hyperfine effect in muonic atoms Hyperfine capture & transition in μ^{-11} B	68		
M15	Hfs resonance in muonium V ₀ resonance test on Mu in SiO ₂			334
M20	μ^+ SR on itinerant magnetism μ^+ SR studies on CoS ₂	52		69
M21	μ^+ SR on spin glasses μ^+ SR on ilmenite hematite & Δu Fe(1.0 af. Z)	210		
M22	Quantum diffusion of μ^+ in Cu ZF- μ^+ SR on Cu from 0.09 K - 200 K	135		
M23	μ^+ SR studies on dense Kondo system μ^+ SR on CeB ₆	44		28
M24	Studies of pulsed muon & muonium spin resonance Time dependent resonance on μ^+ in MnO Resonance hunting & testing	74	203	
M25	μ^+ SR studies on valence fluctuating system μ^+ SR on Sm ₂ Se ₃	40		
M26	Chemical analysis by atomic μ^- capture μ^- capture in organic compounds C _x H _y C _z & C _x H _y S _z	4	196	
M27	μ^+ trapping by extended defects in metals μ^+ SR in irradiated Al with voids			23
M28	Pulsed laser resonance spectroscopy μ reaction with NO ₂ in Ar			61
M29	μ^+ SR studies on magnetism with competing ordering μ^+ SR on Fe _{1-x} Co _x			56

If those are completely performed, the present neutron intensity will be increased by one order of magnitude. Some of them are already completed or under way as mentioned.

While the KENS-I' program is in progress, a long-term future program of BSF has been discussed on the basis of the encouraging results obtained by both of the neutron scattering experimental facility KENS and the pulsed muon facility BOOM in BSF. This is the construction of a more intense pulsed neutron source, KENS-II program, and the extension of the present pulsed muon facility, Super BOOM project. The central facility of this future program is an 800 MeV rapid-cycling proton synchrotron, GEMINI, which intends to deliver pulsed proton beams of 500 μ A in time average. The design studies of this accelerator are in progress. Details of the design are presented in this meeting⁸⁾.

References

- 1) C. W. Schmidt and C. D. Curtis, IEEE Trans. Nucl. Sci., NS-26, 4120, 1979.
- 2) S. Fukumoto, et al., ISIAT '81, 223, 1981, and IEEE Trans. Nucl. Sci., NS-28, 2693, 1981.
- 3) K. N. Leung and K. W. Ehlers, Rev. Sci. Instrum., 53 803, 1982.
- 4) S. Fukumoto, to be submitted to ISIAT '83.
- 5) Y. Ishikawa, et al., presented paper to this meeting.
- 6) Y. Ishikawa, N. Niimura, and S. Ikeda, ed., KENS Report-IV, KEK Internal (1983).
- 7) Meson Science Lab., Univ. of Tokyo, UT-MSL Newsletter No. 1, 1981 and No. 2, 1982.
- 8) H. Sasaki, et al., presented paper to this meeting.

matters and also used to measure the μ^+ motion in metals, muonium chemical reactions, etc. In particular, with pulsed muons which have strong advantage for long time range measurement, one can now measure low frequency muon spin rotation, long μ^+ spin relaxation, slow muonium chemical reactions, μ^+ fast diffusions, etc. Moreover, the pulsed muon beam with low duty factor can introduce the magnetic spin resonance technique, in which high RF field (closed to 100 kW peak power) is required to complete muon spin transition within muon life time.

Thus, the pulsed μ SR experiments cover a wide range of research field. Active experiments in the pulsed muon facility BOOM are listed in Table 5.

Future Program

KENS-I' program of the neutron scattering facility in BSF is a project up-grading the present existing accelerator and experimental facilities in a short period. The major items of the improvement in the program are as follows.

- 1) Conversion of injection scheme in the booster synchrotron from the multi-turn injection of proton beam to H⁻ charge-exchange injection.
- 2) Energy-up of the 20 MeV injector linac to 40 MeV.
- 3) Conversion of the present tungsten target for spallation neutron production to a depleted uranium target.
- 4) Adoption of a grooved-surface solid methane moderator, etc.